

## Analysis of Thermomechanical Stress Induced in Silicon Heterojunction Solar Cells by Copper Fingers

Pei-Chieh Hsiao<sup>1</sup>, Jack Colwell<sup>2</sup>, Daniel Chen<sup>2</sup>, Chris Huang<sup>2</sup>, Alison Lennon<sup>1,2</sup> and Renate Egan<sup>1</sup>

<sup>1</sup> School of Photovoltaics and Renewable Energy Engineering, UNSW, Sydney, Australia, 2052

<sup>2</sup> SunDrive Solar Pty Ltd, Kirrawee, NSW, Australia, 2232

E-mail: [p.hsiao@unsw.edu.au](mailto:p.hsiao@unsw.edu.au)

### Abstract

A world record cell efficiency of 26.81% for crystalline solar cells has been achieved using silicon heterojunction (HJT) technology. The increased Ag usage per cell compared to PERC and TOPCon cells has motivated efforts to develop alternative copper (Cu) metallisation for HJT cells. Copper electrodeposition through a patterned mask is a low-cost room-temperature process. Annealing of copper-plated contacts occurs during subsequent processing steps, including hydrogenation and module fabrication (namely interconnect soldering and lamination). Due to the different thermal and mechanical properties between silicon (Si) and Cu, thermomechanical stress can be induced during these thermal processes. This work presents a finite element analysis of induced stress due to Cu fingers formed on pyramidal textured Si surface undergoing thermal processes.

### Supporting Information

The material properties used in the finite element modelling (FEM) are summarised in Table 1. Monocrystalline Si is anisotropic and hence modelled by a stiffness matrix. The 100 nm-thick indium tin oxide (ITO) layer is treated as a linear elastic material. The material properties of plated Cu are inferred to be identical as solid Cu, and hence a multilinear kinematic hardening model is used for the Cu structures. Both yield strength and coefficient of thermal expansion (CTE) are temperature dependent.

**Table 1 Material properties for FEM of Cu annealing process**

Material	Young's modulus (GPa)	Yield strength (MPa)	Poisson's ratio	Density (kg/m <sup>3</sup> )	CTE (10 <sup>-6</sup> K <sup>-1</sup> )	Thickness (μm)
Si	Anisotropic [1]	-	0.28	2329	T-dependent	160
ITO	92 [2]	-	0.33	6560	7.2 [3]	0.1
Cu	Multilinear [4] (T-dependent)	T-dependent [4]	0.35	8960	T-dependent [5]	8

The textured surface was modelled by uniform pyramids with a base length of 1.5 μm and a facet angle of 54.7°. As shown in **Figure 1** (a), the model geometry covered an area of 100 x 54 μm and consisted of sharp pyramids, with rounded pyramidal edges and apices (radius of 0.06 μm, see **Figure 1** (b)) being used in the regions of interest to avoid stress singularities. Zero directional displacement (dz) was assumed in the thickness direction at the Si centre, and hence half-thick Si was included due to symmetry. The thickness of the Cu fingers was fixed at 8 μm while the width was varied during simulations. To represent the properties of the plated Cu structures, round corners were used for the Cu cross sections. It is known that the pyramidal faces are aligned with the (111) Si crystal plane and the base edges are along the (110) direction. Therefore, the Cu contact edge may be positioned at different distances from pyramid apices as illustrated in **Figure 1** (c). Hence, a normalised distance  $\hat{d}$  was defined as

$$\hat{d} = \frac{d}{p/\sqrt{2}}$$

where  $d$  is the distance of the Cu contact edge to the nearest pyramidal apex under the contact and  $p$  is the pyramid size.

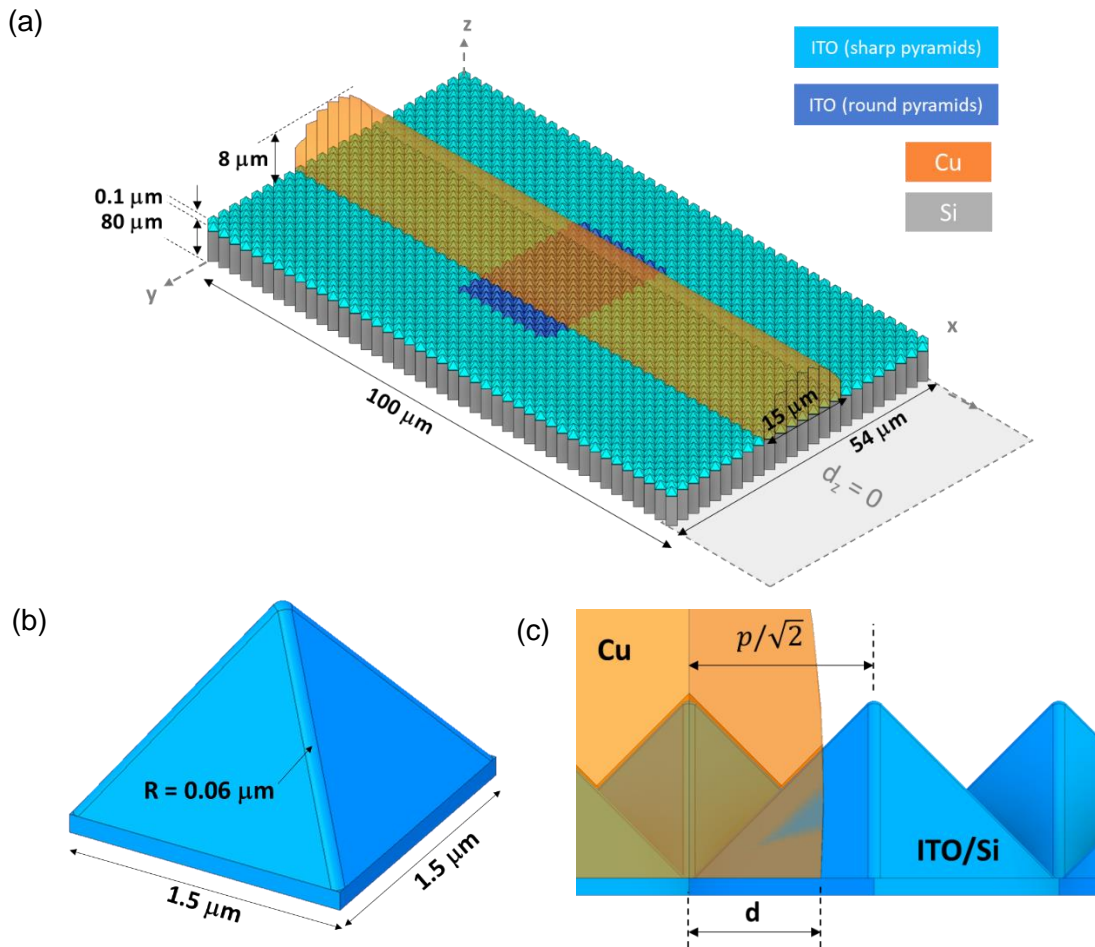


**Figure 1. Schematic diagram showing (a) model geometry; (b) rounded pyramid; and (c) the edge of Cu finger contacting the pyramidal ITO/Si surface.**

The peak annealing temperature was set to 200 °C and homogenous temperatures were assumed for all materials. The induced stress and strain were evaluated both at the peak temperature and after cooling to 20 °C.

Impact of plated Cu edge location

**Figure 2** shows the Si 1<sup>st</sup> principal stress induced by a 15 μm-wide Cu finger after heating to 200 °C and after cooling to 20 °C. When temperature increased from 20 to 200 °C, the Cu finger expanded more than Si due to Cu’s higher CTE. In the centre of the Cu finger, the Si stress tensor was dominated by hydrostatic stress, resulting in primary changes in volume than shape. Therefore, lower stress was induced in the Si under the middle of the finger. At the pyramids near the contact edges, the stress tensor on the two outer pyramidal surfaces was lower than the two inner counterparts owing to the decreased Cu volume. Hence, the maximum 1<sup>st</sup> principal stress was concentrated at the pyramidal apices on the inner surfaces where the directional changes of stress tensor were higher. At the centre of the Cu finger, stress up to 30 MPa penetrated ~ 2.7 μm into the Si bulk.

As with the heating process, hydrostatic stress dominated the Si stress tensor near the finger centre when cooling from 200 to 20 °C, resulting in Si stress reducing under the middle of the finger. As the Cu had deformed plastically during heating with high local strain along the contact edge, maximum stress relaxation occurred in Si when dropping to 70 °C. Below 70 °C, Cu contracted further than Si,

leading to the higher stress at the pyramidal edges perpendicular to the finger direction, which also extended outside the contact regions due to locally deformed Cu with high strain. As shown in **Figure 2 (b)**, the stress penetration was primarily formed outside the finger contact with a decreased penetration depth after cooling.

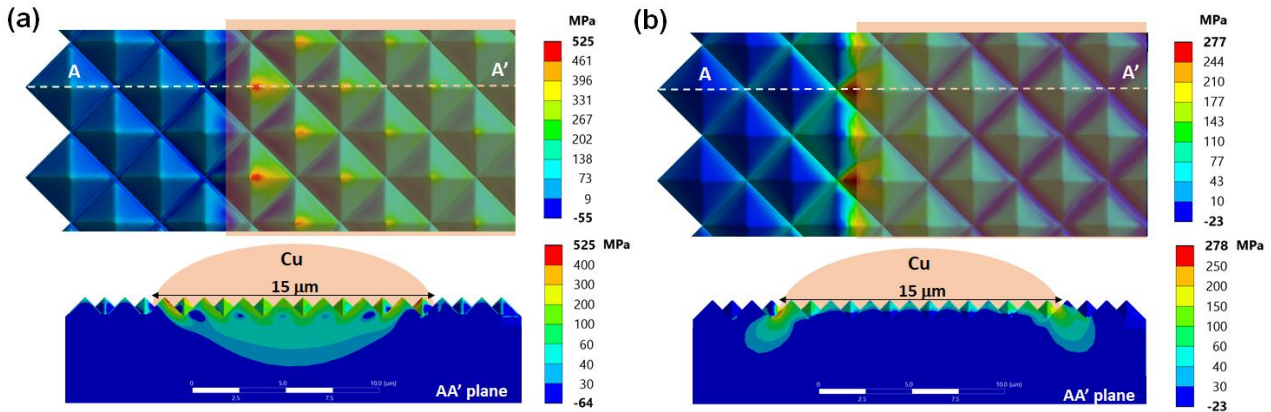


**Figure 2. Simulated Si 1st principal stress induced by 15- $\mu\text{m}$  wide Cu finger subjected to 200 °C annealing (a) at 200 °C and (b) after cooling at 20 °C. The plated Cu location was  $\hat{d} = 0.6$ .**

The impact of contact location ( $\hat{d}$ ) of the Cu finger on the maximum Si stress is graphed in **Figure 3**. The red curve shows that induced Si stress at the peak temperature was consistent at  $509 \pm 17$  MPa regardless of the contact location. On the contrary, Si stress after annealing generally decreased with  $\hat{d}$  as the imbalance of stress tensors was reduced at large  $\hat{d}$ , leading to a stress range of 77 MPa.

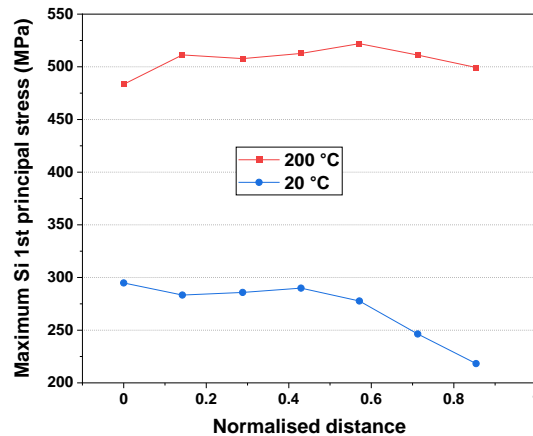


**Figure 3. Simulated maximum Si 1st principal stress induced by a 15- $\mu\text{m}$  wide plated Cu subjected to 200 °C annealing as a function of normalised distance  $\hat{d}$ .**

**Figure 4** shows the von Mises stress and equivalent total strain of the Cu finger. At 200 °C, the local maximum Cu stress and strain occurred at the contact edge [see **Figure 4(b)**], resulting in a slight dependent on  $\hat{d}$ . After cooling, the maximum strain in the Cu finger was located at the pyramidal apices and consistent Cu stress occurred at all contact faces. Therefore, the impact of  $\hat{d}$  was insignificant.

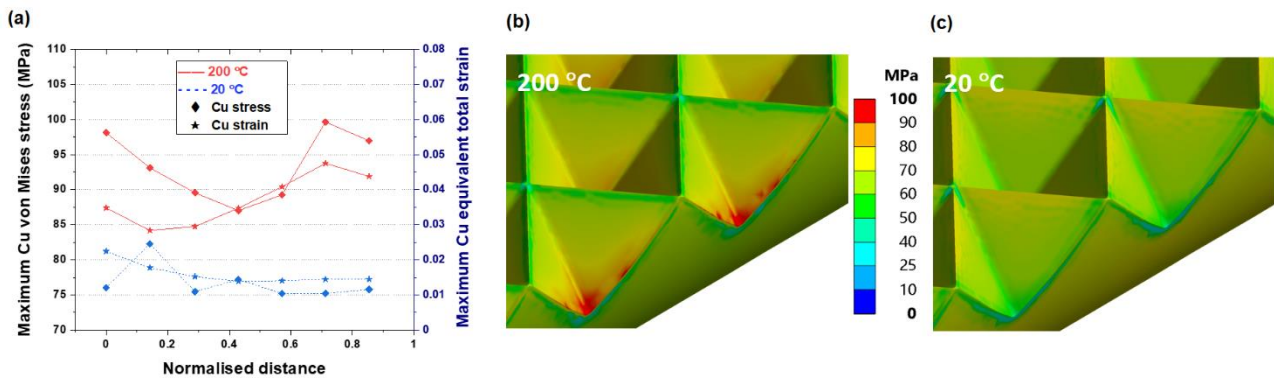


Figure 4. Simulated maximum von Mises stress and equivalent total strain of a 15- $\mu\text{m}$  wide Cu finger subjected to 200  $^{\circ}\text{C}$  annealing (a) as a function of contact location  $\hat{d}$ , (b) stress at 200  $^{\circ}\text{C}$  and (c) stress at 20  $^{\circ}\text{C}$ .

### Impact of Cu finger width

The simulated Si stress induced by Cu fingers with a width ranging from 7.5 to 100  $\mu\text{m}$  is shown in **Figure 5**. The maximum Si 1<sup>st</sup> principal stress increased with Cu finger width and became stabilised at  $\geq 50 \mu\text{m}$ . Additionally, the stress depth penetration was found to be positively correlated with the maximum stress values. The results indicate that larger finger width introduced greater stress range. When the finger width was  $\geq 50 \mu\text{m}$ , a consistent local stress was induced at the pyramidal edge near the apex. If the finger edge coincided with this local stress point, then the Si stress magnitude was increased. Consequently, narrow fingers are advantageous in both reducing optical shading and thermomechanical stress in Si. As the absolute stress values depend on the constitutive models used in the simulations, direct characterisation of the material properties of plated Cu would predict results with high fidelity. Further investigation is also required to evaluate the impact of such highly localised stress in the sub-micron scale.

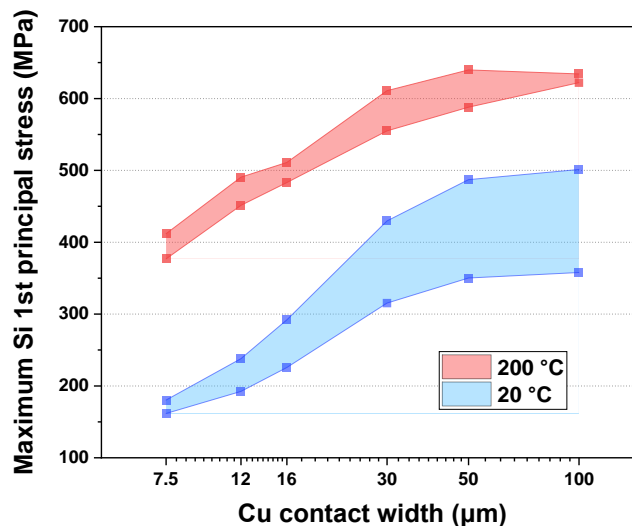


Figure 5. Simulated maximum Si 1st principal stress induced by Cu fingers of varying width. The stress range was simulated by varying  $\hat{d}$  from 0 to 0.9.

The influence of Cu finger width on its maximum stress and strain is shown in **Figure 6**. Simulated Cu stress and strain at 200  $^{\circ}\text{C}$  clearly increased with the finger widths, however there was no apparent difference after cooling back down to 20  $^{\circ}\text{C}$ .

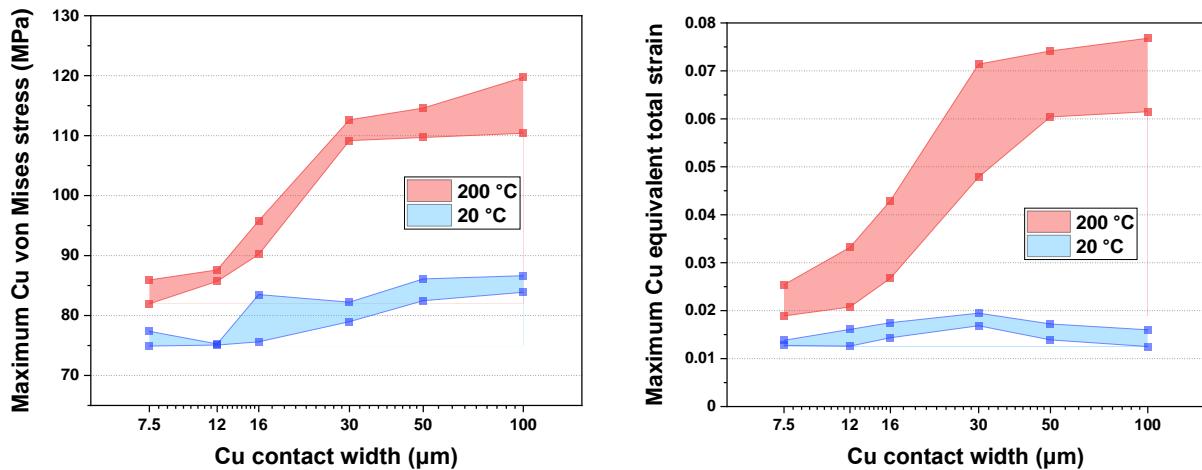


Figure 6. Simulated maximum Cu von Mises stress and equivalent total strain of Cu fingers with varying widths. The stress and strain range was simulated by varying  $\tilde{d}$  from 0 to 0.9.

## Conclusion

Thermomechanical stress induced by annealing of Cu fingers on pyramidal textured HJT cells was analysed. The finite element simulation showed that maximum Si stress was influenced by the location of the finger relative to the pyramidal apex and the finger width. The maximum stress location in Si transited from the pyramidal apexes at peak temperature to the finger edges after cooling. Meanwhile the primary stress penetration changed from the finger centre to outside the finger. Maximum Si stress not only increased with the finger width, but also the induced stress range increased. On the other hand, the maximum von Mises stress and equivalent total strain of Cu fingers remained similar regardless of the contact location and finger width.

## Acknowledgement

This work has been supported by the Australian government through the Australian Renewable Energy Agency (ARENA) and the Australian Centre for Advanced Photovoltaics (ACAP). This project has been supported by the NSW Government through its Environmental Trust.

## References

- [1] J. J. Hall, "Electronic Effects in the Elastic Constants of n-Type Silicon," *Physical Review*, vol. 161, no. 3, pp. 756-761, 09/15/ 1967.
- [2] T. Wittkowski, J. Jorzick, H. Seitz, B. Schröder, K. Jung, and B. J. T. S. F. Hillebrands, "Elastic properties of indium tin oxide films," vol. 398, pp. 465-470, 2001.
- [3] H. Kim *et al.*, "Effect of film thickness on the properties of indium tin oxide thin films," vol. 88, no. 10, pp. 6021-6025, 2000.
- [4] R. Sandström, J. Hallgren, and G. Burman, "Stress strain flow curves for Cu-OFP," 2009.
- [5] K. Wang, R. R. J. H. t. Reeber, and m. science, "Thermal expansion of copper," vol. 35, no. 2, 1996.